Proceedings RootS25
3rd International Workshop on Soil-Vegetation-Atmosphere Interaction
Boldrin D, Cecconi M, Cotecchia F, Leung A, Pedone G, Perrini P, Romero E, Tagarelli V, Zdravković L (eds)
ISSN: 3107-300X

doi: doi.org/10.53243/RootS2025-36

Sensitivity analysis of the thermo-hydraulic parameters characterizing vegetation in an evapo-transpiration model

Nico Stasi[1], Silvano Emanuele Donvito[1], Vito Tagarelli[1], Jean Vaunat[2], Federica Cotecchia[1]

[1]*Department of Civil, Environmental, Land, Building Engineering and Chemistry, Politecnico di Bari, Italy*
[2]*Department of Civil and Environmental Engineering, Universitat Politècnica de Catalunya, Barcelona, Spain*

ABSTRACT: Nature-based solutions (NBS) are increasingly recognized as effective strategies for mitigating weather-induced landslides. Among the key mechanisms, vegetation can enhance slope stability by regulating the energy and water balances through evapotranspiration (ET), which lowers pore water pressure and consequently reduces landslide risk.
This study investigates the sensitivity of ET estimates to variations in vegetation constitutive properties within a physically based thermo-hydraulic framework. A Python-based tool was developed to perform back-analysis and sensitivity analyses under different meteorological conditions, quantifying the influence of vegetation-specific parameters on ET dynamics.
The application focuses on a clayey soil cover in a landslide-prone area, where the engineered vegetation mix Prati Armati® (Poaceae species) has been introduced. By systematically varying input parameters across different growth stages, we delineate theoretical ranges of ET fluxes associated with these species.

Keywords: Soil-vegetation-atmosphere interaction, Nature-Based Solutions, Evapotranspiration, Numerical analysis, sensitivity analysis

1 INTRODUCTION

The interaction between soil, vegetation, and the atmosphere, SVA, plays a fundamental role in the equilibrium conditions of geotechnical systems. Indeed, the processes part of the SVA interaction control the water and energy exchanges between the geotechnical system (from top to underground soils), the distribution of soil moisture and temperature across the system and, hence, the thermo-hydro-mechanical, THM, state of the soils.

Vegetation acts within the SVA interaction through leaf interception, shading, root water uptake, transpiration and plant-controlled energy fluxes (Stasi et al., 2024). Hence, advanced modelling of SVA interaction requires the simulation of the processes controlled by vegetation and is essential to support the use of plants as nature-based solution, NBS, for the mitigation of landslide activity and erosion. To this aim, finite element, FE, models have been extended to include the plant processes, according to different strategies (e.g., Samat, 2016). However, the sensitivity of such models to plant-specific parameter variability remains insufficiently assessed, even though vegetation traits vary across species, ecosystems, and climates. Parameter values should therefore be species-specific and calibrated to local climatic and site conditions; in parallel, sensitivity analyses are needed to identify which parameters and ranges most influence predictions of evapotranspiration (ET) and energy fluxes. Model predictions must also be checked against benchmark ET estimates from analytical (e.g., energy balance, EB) to verify that simulations remain physically consistent.

This paper addresses these needs with two complementary studies, both carried out over a typical monitoring year (2024) using the formulation implemented in the FE code Code_Bright (Olivella et al., 1996). This kind of eco-physiological model has been preferred to more widely used semi-empirical models (e.g. FAO Penman–Monteith), since it allows for greater control over the parameters involved and enable a more detailed assessment of the effects of plant development and soil moisture condition.

The analyses have been run to simulate a prototype soil, plant and climatic conditions, making reference to a pilot site in the south-eastern Italian Apennines, where a turbiditic clayey topsoil covers a slope, location of deep weather driven landslide activity (Tagarelli & Cotecchia, 2022). Part of the test site has been seeded with selected vegetation, and the topsoil has been instrumented (down to 2.5 m depth) to monitor the SVA interaction (Stasi, 2024). This setup enables EB-based ET estimates for benchmarking (Stasi et al., 2025) and supplies the SVA dataset required for model calibration, back-analysis, and sensitivity assessment.

This work highlights the model's ability to predict ET across plant growth stages and to guide the implementation of vegetation layers in finite-element SVA models, providing reference benchmarks for validating parameter values in empirical ET methods such as the FAO Penman-Monteith approach.

2 MATERIAL AND METHODOLOGY

The set of equations adopted in Code Bright to simulate the evaporation, E, and the transpiration, T, fluxes, has been implemented in Python to perform two analyses.

As first, we perform a back-analysis of ET fluxes, comparing the model predictions with an EB benchmark (Stasi et al., 2025). In this back-analysis, the vegetation is modelled by a set of plant-specific parameters derived from laboratory and in-situ evidence for the stages: Early, Mid, Late (Stasi 2024).

Second, we performed a global sensitivity analysis using Partial Rank Correlation Coefficients (PRCC), which quantify the monotonic influence of each input on ET while accounting for concurrent variation in the others through rank-based partial correlations (Saltelli et al., 2008). Parameter ranges for vegetation were selected from literature for Poaceae vegetation, whereas meteorological inputs were sampled within stage-specific ranges observed in-situ.

The formulation adopted in the code computes E and T as fluxes, accounting for meteorological action, vegetation properties, and soil hydraulic conditions following the scheme in Fig.1. In particular, E and T are obtained as fluxes driven by the vapour density gradients between soil and the atmosphere (Fig. 1) as follows:

$$E = \frac{1-veg}{r_a}\left(\rho_{v,atm} - \rho_{v,\mathrm{soil}}\right) \quad (1)$$

$$T = \frac{veg}{r_a + r_s}\left(\rho_{v,atm} - \rho_{v,\mathrm{soil}}\right) \quad (2)$$

where r_s and r_a are respectively the surface and aerodynamic resistance, veg is the vegetated fraction (i.e. surface covered by vegetation for unit area of ground, 0-1) and $\rho_{v,atm}$ and $\rho_{v,\mathrm{soil}}$ are the vapour density in the atmosphere and in the soil, respectively. The soil surface resistance, $r(\rho_{v,soil})$, in both saturated and unsaturated zones, was considered in the vapour density calculation.

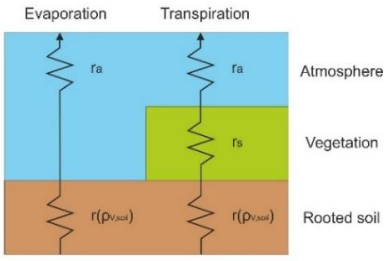

Figure 1. Schematic representation of the resistive pathways for vapour diffusion within the SVA continuum. The system is conceptualized as a one–dimensional series of resistances

The meteorological input consists of time series of shortwave solar radiation (R), air temperature (T_a), relative humidity (RH), wind speed (u), and atmospheric pressure (p_{atm}), all recorded on site at 15-minute intervals. Soil state variables included near-surface soil temperature (T_s) and volumetric water content (θ) also obtained from in situ monitoring. From these, the soil saturation S_r was derived as S_r=θ/n, with n representing the porosity of the soil. The vapour pressure deficit (VPD) was also computed from T_a and RH by using the psychrometric law.

Surface and aerodynamic resistance are computed as:

$$r_s = \frac{r_{s,min}}{LAI}\left(\frac{F1}{F2\ F3\ F4}\right) \quad (3) \qquad r_a = \frac{ln(z_a/z_0)^2}{k^2\ \varphi\ u} \quad (4)$$

and are related specifically to the vegetation and the atmosphere, respectively. In particular, r_a is estimated based upon the wind speed, u, the roughness length, z_0, the reference height, z_a, and stability factor, φ, (kept constant). On the other hand, the r_s, is computed based upon quantities that refer to both the vegetation and the soil, and is limited by four different functions, F_1, F_2, F_3 and F_4, which account for photosynthetically active radiation, soil moisture, vapour pressure deficit, and temperature, respectively. These functions are computed as:

$$F_1 = \left[1 + \left(\frac{1.1}{LAI}\ \frac{R_G}{R_{GL}}\right)\right] \Big/ \left[\left(\frac{1.1}{LAI}\ \frac{R_G}{R_{GL}}\right) + \left(\frac{r_{s,min}}{r_{s,max}}\right)\right] \quad (5)$$

$$\frac{F_2}{RDen} = \begin{cases} 0 & if\ Sr \le Sr_w \\ \frac{Sr - Sr_w}{Sr_{FC} - Sr_w} & if\ Sr_w < Sr \le Sr_{FC} \\ 1 & if\ Sr_{FC} < Sr \le Sr_{AN} \\ \frac{1-Sr}{1-Sr_A} & if\ Sr > Sr_{AN} \end{cases} \quad (6)$$

$$F_3 = 1 - \gamma\left(P_{v,sat} - P_v\right) \quad (7)$$

$$F_4 = exp(-0.0016\ (298 - T_{atm}))^2 \quad (8)$$

with all these parameters are defined in the following.

Soil hydraulic properties were represented using the van Genuchten (1980) retention model, defined by residual and saturated water contents, θ_r and θ_s, porosity, and the shape parameters α and n. Suction Pc was related to S_r through the effective saturation S_e, and the Kelvin equation was then applied to compute the vapour density at the soil surface, $\rho_{v,soil}$, limiting upward vapour and liquid flow. The atmospheric vapour density, $\rho_{v,atm}$, was calculated from T_a and RH.

The vegetation was parameterized by a set of descriptors depending on the growth stage (Early, Mid, Late), including: the leaf area index, LAI; minimum and maximum stomatal resistances, $r_{s,min}$ and $r_{s,max}$; radiation parameter, R_{gl}; soil moisture thresholds for water stress, $S_{r,w}$, $S_{r,fc}$ and $S_{r,a}$; empirical correction factors for temperature, a_4; vapour pressure, γ^{-1}; vegetation density, r_{Den}; fractional vegetation cover, veg; roughness length, $z_{0,m}$; stability factor, stabfac. These parameters, listed in Table 1, were derived from both laboratory and site measurements, and when not available, from literature.

The back-analysis has been run by applying the meteorological and the soil state logged in the field as input of the model (Figure 1). The results of the model in term of the E and T fluxes are reported and discussed later.

As for the second analysis, the Partial Rank Correlation Coefficient (PRCC) method was adopted for the parametric sensitivity analysis, as it quantifies the effect of varying a given input parameter on the predicted ET while accounting for simultaneous variations in all the

others (Saltelli et al., 2008). The variation ranges for the vegetation parameters were defined from literature data for Poaceae. Meteorological parameters were sampled within ranges representative of the monitored records at Pisciolo, with distinctions introduced among the three vegetation growth stages observed in the field. This approach enabled PRCC to disentangle and quantify the relative influence of species–specific traits and climatic forcing on the ET estimates. The adopted variability ranges parameters are in the legend of Figure 3.

Table 1. Parameters adopted for the parametric analysis

Parameter	Early (Nov–Apr)	Mid (May–Jun)	Late (Jul–Oct)
LAI (–)	0.5	1.5	1.0
Z_0	0.02	0.05	0.2
$r_{s,min}$ (s m^{-1})	50	60	100
$r_{s,max}$ (s m^{-1})	5000	4000	3000
R_{GL} (W m^{-2})	130	130	100
Sr_w (–)	0.25	0.08	0.08
Sr_{FC} (–)	0.9	0.9	0.9
Sr_{AN} (–)	0.9	0.99	0.99
r_{Den} (–)	0.20	0.70	1.00
γ^{-1} (MPa^{-1})	40	30	25
a_4 (–)	0.006	0.002	0.0005
veg (–)	0.30	0.75	0.90

3 RESULTS

Figure 2 illustrates only the results for a representative day, extracted within the *Mid* growth stage. Figure 2a reports the weather input data. The net radiation, R_{net}, varies as expected for the diurnal cycle, with peaks exceeding 600 W*m^{-2}, while T_a rises to approximately 22 °C during daytime. T_s (soil) follows a smoother trend, while Sr remains nearly constant, indicating near-saturated soil conditions with suction values of 300 KPa. Figure 2b shows the functions F_1–F_4, which govern the transpiration flux. The solar radiation function F_1 remains high during night-time and exhibits a sharp decrease as the radiation increases during the daytime. In contrast, F_2 and F_3 remain almost constant, because variation in controlling variables is limited over the one-daytime. F_4 exhibits only a slight variation, consistent with the temperature fluctuation over the day. It can be concluded that, under the examined conditions, in a single day the variability of ET is largely governed by the excursion of incoming solar radiation, rather than by changes in the soil TH conditions.

Figure 2c reports a comparison between the simulated fluxes of transpiration, evaporation, and their sum, i.e. total ET, with the ET flux deduced through the energy balance, EB, method applied to the data monitored in the field, called measured ET in the following. The predicted ET reproduces both the magnitude and diurnal variability of the measured ET, with values typically ranging between 0.05 and 0.15 mm/15min. Despite a vegetation cover of 75% is assumed, E dominates the total flux, while the resistance r_s characterizes a strong stomatal control and the aerodynamic resistance, r_a, remains comparatively low and stable. The comparison with fluxes derived from the EB method suggest that with this setting, the model tends to underestimate the ET fluxes, particularly until midday. Nevertheless, it reproduces the overall trend quite well.

Figure 3 summarizes the results of the PRCC sensitivity analysis, and the range of variability adopted for the parameters in the second part of the study. Each horizontal bar represents the correlation coefficient, CC, for a single input parameter, computed while statistically controlling for all other inputs. Across all growth stages (that refer only to the weather forcing monitored in-situ), vegetation cover, veg, emerges as the parameter best correlated to ET among the vegetation parameters (CC $>$ 0.5 in the early stage and $>$ 0.6–0.7 in the mid/late stages). Among soil and meteorological variables, T_s and R_{net} exert the largest positive control (≈0.4–0.6, depending on the stage). LAI also contributes positively (≈0.25–0.45), though consistently secondary to veg. RH and T_a show strong, monotonic negative CCs (often $<$–0.4, reaching –0.6 to –0.7), indicating that, higher RH (i.e., lower vapor pressure deficit, VPD) and higher T_a are associated with lower ET. This is consistent with stomatal closure under increased atmospheric stress and the dampening effect of low VPD on vapor fluxes. R_{Den} contributes positively (≈0.2–0.4), particularly in the mid-to-late stages, in line with enhanced water supply and canopy development. Stomatal parameters within F_1 (i.e., $r_{s,min}$ and $r_{s,max}$) exhibit negative CCs (small-to-moderate bars to the left), as expected since larger resistances reduce canopy conductance and ET. Conversely, LAI, also part of F_1, shows positive CC values, reflecting the increase in conductance with leaf area. The radiation parameter R_{GL} displays near-zero to slightly positive CCs across stages, indicating a minor impact. This is explained by the slight variability in the R_{GL} range for the incoming radiation, and by the fact that light is rarely limited during peak hours, making R_{net} the dominant driver.

Since CC captures only monotonic influences, it underestimates parameters that act through interactions. for instance, the atmospheric stability factor, although crucial for energy-balance ET estimation, shows low partial influence here due to its strong correlation with dominant radiation and aerodynamic terms.

4 CONCLUSIONS

The application of the model using real field data allowed a realistic observation of the magnitude of daily ET flux variability in relation to atmospheric forcing.

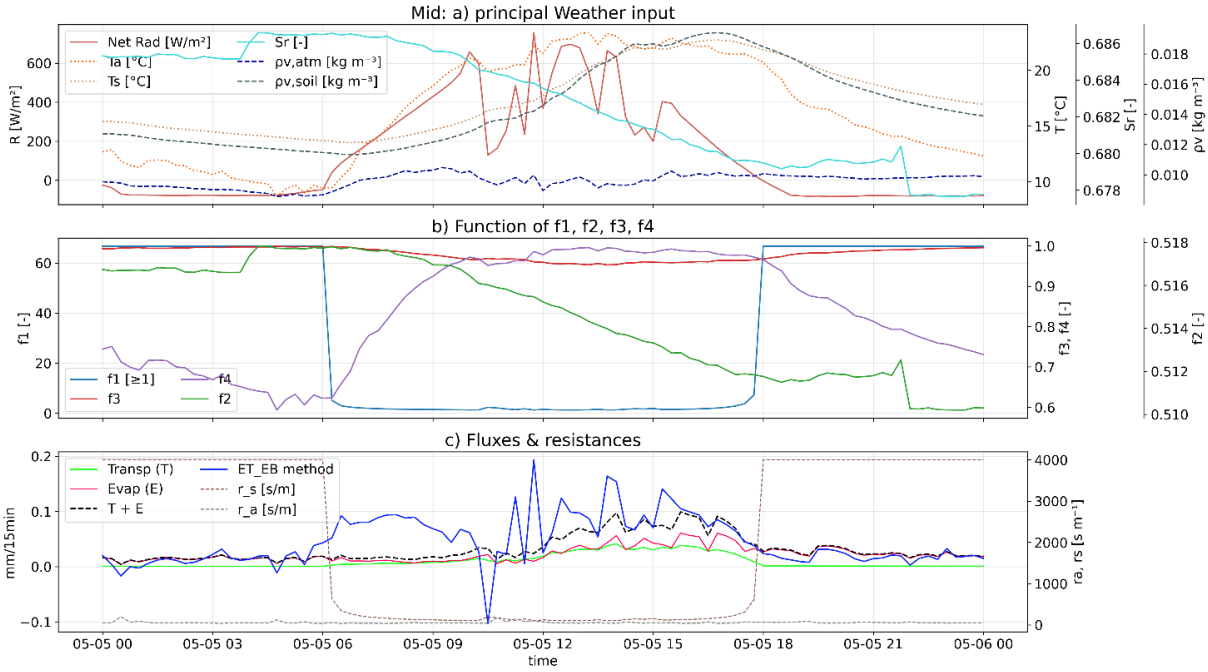

Figure 2. Evolution over a single representative day within the Mid growth stage of the input variables (a) and results (b and c) of the parametric Python analysis

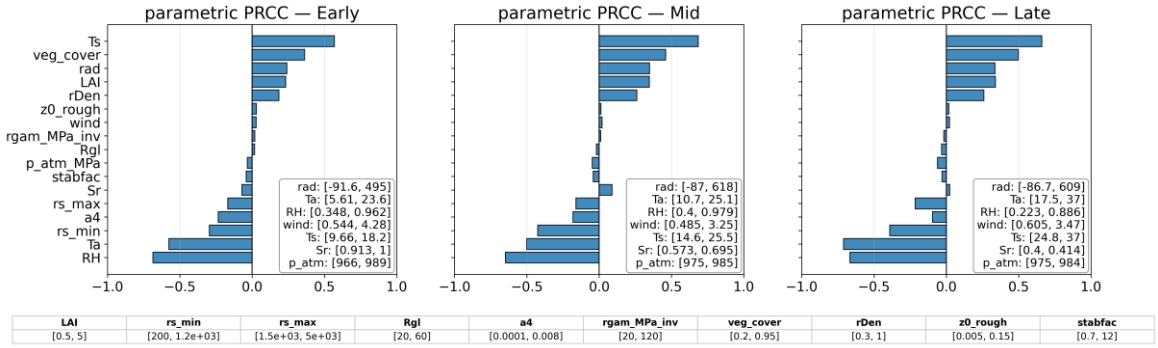

Figure 3. Results of the PRCC sensitivity analysis for the different stages in the year

However, the comparison with field measurements highlights the need for a more refined calibration of vegetation properties, supported by site specific investigations. In this regard, the results of the sensitivity analyses provide key insights and priorities for parameter selection and benchmarking.

Future work will include validating the vegetation module in Code Bright to enable reliable coupled predictions of soil response and infiltration processes.

5 ACKNOWLEDGEMENTS

This research was funded by project PNRR, MISURA M4_C2_1.4, (CN_00000013 CUP: D93C22000430001) Spoke 5 “Environment and Natural Disasters”.

6 REFERENCES

Olivella, S., Gens, A., Carrera, J., Alonso, E. 1996. Numerical Formulation for a Simulator (CODE_BRIGHT) for the Coupled Analysis of Saline Media, *Engineering Computations* **13**(7), 87–112.

Saltelli, A., Ratto, M., Andres, T., Campolongo, F., Cariboni, J., Gatelli, D., Saisana, M., Tarantola, S. 2008. Global Sensitivity Analysis, *The Primer*, Chichester, UK.

Samat, S. 2016. *Thermomechanical Modelling of Ground Response Under Environmental Actions.* PhD Thesis, Universitat Politècnica de Catalunya.

Stasi, N. 2024. *Experimental and numerical study of Soil-Vegetation-Atmosphere interaction for the design of Nature-Based Solutions in landslide risk mitigation.* PhD Thesis, University of Bari.

Stasi, N., Tagarelli, V., Cafaro, F., Cotecchia, F. 2025. Thermo-hydro-mechanical field monitoring of a clayey topsoil: insights of the soil-vegetation-atmosphere interaction. *9th ISGSR.* Oslo, Norway

Stasi, N., Tagarelli, V., Cafaro, F. The impact of a wildfire on a vegetated topsoil: field monitoring and numerical modelling, *CUTE 2024*, Poland, Wrocław.

Tagarelli, V., Cotecchia, F. 2022. Preliminary field data of selected deep-rooted vegetation effects on the slope-vegetation-atmosphere interaction: results from an in-situ test, *Italian Geotechnical Journal*, 1/2022, 62-83.